$$K_1 = Z[\exp(-\Delta A_1/RT) - 1] \quad (9)$$

Here K_1 is expressed in mole fraction units, Z is the quasi-lattice coordination number, and ΔA_1 is the change in total acceptor-donor interaction energy, including the free energy contribution from changes in internal degrees of freedom for the thiocyanate ion. Analogous expressions can be derived for any step:

$$Cr(NCS)_{Z-j+1}F_{j-1}^{3-} + F^- \rightarrow Cr(NCS)_{Z-j}F_j^{3-} + SCN^-$$

In this system, where the complexation (i.e. the tendency to nonrandom anion distribution) is strong, it holds that $\exp(-\Delta A_j/RT) \gg 1$ for all values of j, so ΔA_j can be calculated according to

$$\Delta A_j = \Delta G^\circ_j + T[\Delta S^\circ_j(\text{conf})] \quad (10)$$

$\Delta S^\circ_j(\text{conf})$ is the ideal configurational entropy change, determined by the statistical probabilities of exchanging SCN^- for F^- in a fixed coordination sphere:

$$\Delta S^\circ_j(\text{conf}) = R \ln \frac{Z - j + 1}{j} \quad (11)$$

In view of the results from our study of ligand field spectra, it seems justified to use a value of 6 for Z. We calculated the total interaction energies ΔA_1-ΔA_4, and it appeared that all energy parameters fall in the range -36 ± 3 kJ·mol^{-1}.

The closeness of all ΔA_j values implies that the overall complexation process might be well described by the use of only one single specific interaction parameter ΔA independent of the number of fluoride ligands attached to the Cr(III) central ion. If so, the stability constants can be estimated through

$$\beta_j^* = \exp\left[\frac{-j(\Delta A)}{RT}\right]\frac{\prod_j(Z - j + 1)}{j!} \quad (12)$$

In Table II the set of β_j^* values, calculated with the best fitting value $\Delta A = -36.4$ kJ·mol^{-1} and $Z = 6$, are included for comparison. The agreement with experimentally determined β values is very good.

These results suggest that the estimated interaction energy may be of more general predictive value. It is thus important to extend the studies of fluoride complexation in mixed KSCN-KF melts to systems with other acceptor ions. Such studies are now in progress at our laboratory.

Acknowledgments. Active support from Dr. Arvid Sandell in the computations is gratefully acknowledged. This work has also been supported by a grant from the Swedish Natural Science Research Council.

Supplementary Material Available: A listing of experimental emf data (4 pages). Ordering information is given on any current masthead page.

Contribution from the Chemical Physics Program, Washington State University, Pullman, Washington 99164-4630

Magnetic Properties and Structural Characterizations of Bis(tetramethylammonium) Decachlorotetracuprate(II) and Bis(4-methyl-2-aminopyridinium) Decachlorotetracuprate(II)

K. E. Halvorson, T. Grigereit, and R. D. Willett*

Received August 14, 1986

The crystal structures of bis(4-methyl-2-aminopyridinium) decachlorotetracuprate(II), $(4MAP)_2Cu_4Cl_{10}$, and bis(tetramethylammonium) decachlorotetracuprate(II), $(TEMA)_2Cu_4Cl_{10}$, have been determined. The 4MAP salt has a monoclinic structure [$a = 3.847$ (2) Å, $b = 21.276$ (2) Å, $c = 15.336$ (6) Å, $\beta = 96.44$ (3)°; space group $P2_1/n$; $Z = 2$] that contains discrete $(C_6N_2H_{10})^+$ cations and pseudoplanar $(Cu_4Cl_{10})^{2-}$ anions. The anions are centrosymmetric bibridged tetramers with each copper(II) ion exhibiting a 4 + 2 coordination geometry. The Cu-Cl distances within the tetramer average 2.285 Å with a range from 2.227 to 2.367 Å. The central Cu-Cl-Cu bridging bond angles are both 93.7°, while the outer pairs are 94.7 and 94.4°. The tetramers form stacks, I, parallel to the a axis, with each copper(II) ion completing its 4 + 2 coordination with chlorine atoms in adjacent

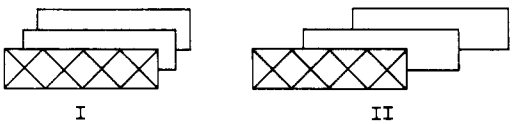

I II

tetramers. The average intertetramer Cu-Cl bond distance is 2.987 Å. $(TEMA)_2Cu_4Cl_{10}$ is monoclinic [$a = 6.072$ (2) Å, $b = 19.574$ (3) Å, $c = 10.617$ (3) Å, $\beta = 99.46$ (2)°; space group $P2_1/c$; $Z = 2$]. This structure also contains discrete $Cu_4Cl_{10}^{2-}$ anions and $N(CH_3)_4^+$ cations. The anions are similar to those of the 4MAP salt, with Cu-Cl distances ranging from 2.215 to 2.346 Å (2.276 Å average) and with central Cu-Cl-Cu angles of 93.5° and terminal angles of 93.6 and 95.5°. The tetramer stacks, II, yield a 4 + 1 coordination geometry for the two end copper(II) ions and a 4 + 2 coordination for the two central copper(II) ions. Magnetic susceptibilities for the salts were fitted to a nearest-neighbor Heisenberg exchange Hamiltonian for a linear tetramer, yielding values of -62.1 (2) K (4MAP) and -59.2 (9) K (TEMA) for the outer coupling constant, J_1/k, and a value of 36 (33) K (4MAP) and 26 (18) K (TEMA) for the central coupling constant, J_2/k.

Introduction

Structural and magnetic properties of copper(II) halide salts have long been of interest in the laboratory. Structurally, the coordination geometry of the copper(II) ions has a very diverse range. In addition, the halide ion is an effective bridging ligand, which imposes few steric constraints upon the coordination geometry. These factors provide a mechanism whereby the magnetic superexchange pathways may be systematically varied.[1] Magnetic properties of these salts have proven to be worthwhile in the study of the spin paramagnetism of pseudo-one-dimensional systems, in which the spins on the metal ions interact via superexchange pathways through the halide ions.[2] Magnetostructural correlations for these salts are also of interest due to the effect of the bridging Cu-X-Cu bond angles and coordination geometry on the value of the magnetic coupling constant.[3]

(1) Ginsberg, A. G. *Inorg. Chim. Acta, Rev.* **1971**, *5*, 45.

(2) Geiser, U.; Gaura, R. M.; Willett, R. D.; West, D. X. *Inorg. Chem.* **1986**, *25*, 4203.

0020-1669/87/1326-1716$01.50/0

Table I. X-ray Data Collection Parameters

compd name	bis(4-methyl-2-aminopyridinium) decachlorotetracuprate(II)	bis(tetramethylammonium) decachlorotetracuprate(II)
empirical formula	$(C_{12}N_4H_{18})_2Cu_4Cl_{10}$	$(C_8H_{24}N_2)Cu_4Cl_{10}$
mol wt	827.015	757.0
diffractometer system	Nicolet R3m/E	Nicolet R3m/E
cryst class	monoclinic	monoclinic
space group	$P2_1/n$	$P2_1/c$
systematic absences	$h0l$, $h + 1 = 2n + 1$; $0k0$, $k = 2n + 1$	$h0l$, l odd; $0k0$, k odd
lattice constants	a = 3.847 (2) Å	a = 6.072 (2) Å
(λ = 0.710 69 Å)	b = 21.276 (2) Å	b = 19.574 (1) Å
	c = 15.336 (6) Å	c = 10.610 (3) Å
	β = 96.44 (3)°	β = 99.46 (2)°
	V = 1255.3 (6) Å^3	V = 1264.9 (5) Å^3
	based on 25 reflcns in the range $19 < 2\theta < 21°$	based on 25 reflcns in the range $33 < 2\theta < 35°$
$F(000)$	808	743.86
radiation	Mo Kα with graphite monochromator	Mo Kα with graphite monochromator
cryst size	0.04 × 0.21 × 0.15 mm^3	0.35 × 0.5 × 0.6 mm^3
abs coeff	44.4 cm^{-1}	44.0 cm^{-1}
ρ_{calcd}	2.19 g cm^{-3} (Z = 2)	1.99 g cm^{-3} (Z = 2)
type of abs corr	numerical	empirical, assuming ellipsoidal shape
max, min transmssn	0.87, 0.63	0.341, 0.236
data collecn tech	ω scan	ω scan
scan range	1°	1°
scan speed: min, max	3.91, 29.3°/min	3.91, 29.30°/min
hkl check reflcns	$12\bar{3}$, 073; monitored every 100 reflcns	012, $01\bar{2}$, 013; monitored every 100 reflcns
total no. of reflcns	1492	3461
2θ(max)	40°	55°
no. of unique reflcns	1144; 843 with $F > 3\sigma(F)$	3054; 2480 with $F > 3\sigma(F)$
R for equiv reflcns	0.0554	0.0490
struct soln package	Nicolet SHELXTL Version 4.1	Nicolet SHELXTL Version 4.1
struct soln tech	direct methods	direct methods
$R = \sum\|\|F_o\| - \|F_c\|\|/\|F_o\|$	0.068	0.038
$R_w = [\sum w(\|F_o\| - \|F_c\|)^2/\sum w\|F_o\|^2]^{1/2}$	0.077	0.035
with $w = 1/[\sigma^2(F) + g(F)^2]$	g = 0.000 52	g = 0.000 06
$\|\Delta/\sigma\|$: mean, max	0.001, 0.003	0.002, 0.016
total no. of params refined	136	110
thermal params	anisotropic on all non-hydrogen atoms	anisotropic on all non-hydrogen atoms
hydrogen atoms	constrained to C–H and N–H = 0.96 Å; thermal params 1.2 times the corresponding heavy atom	constrained to C–H and N–H = 0.96 Å; thermal params fixed at 0.10
largest peak on final diff map	0.7 e/Å^3 near Cl(4)	0.7 e/Å^3 near Cu(2)
extinction corr	none	yes
goodness of fit	2.06	1.576

As part of our program to produce new one-dimensional magnetic systems, several $ACuCl_3$ compounds with strong antiferromagnetic interactions were synthesized with A being a methylaminopyridinium cation.[2] In particular, for n = 4 and 6, the n-methyl-2-aminopyridinium (≡nMAP) salts yielded bibridged chains having a square-pyramidal coordination geometry with J/k = −48 K (n = 4) and −55 K (n = 6). Attempts to synthesize the corresponding n = 3 and n = 5 salts lead to the formation of $(n\text{MAP})_2Cu_3Cl_8$ salts, which contain bibridged, pseudoplanar $Cu_3Cl_8^{2-}$ anions.[4] Attempts to make the corresponding n = 4 salt resulted in the formation of one of the compounds reported in this paper, $(4MAP)_2Cu_4Cl_{10}$. No corresponding oligomeric salt was found with n = 6.

The triangular phase diagram of tetramethylammonium chloride [≡(TEMA)Cl] and $CuCl_2$ in HCl was investigated for several reasons. We are interested in the structural properties of two of the known compounds in this system, $(TEMA)_2CuCl_4$[5] and $(TEMA)CuCl_3$.[6] The dimeric system $HCuCl_3 \cdot 3H_2O$ exists in the $CuCl_2$/HCl end member. The former contains an incommensurate phase near room temperature. The trichloride contains a Jahn–Teller-distorted tribridged chain structure that undergoes phase transitions just above room temperature that may lead to an incommensurate phase. In the process of synthesizing these various compounds, we obtained a new phase of stoichiometry $(TEMA)_2Cu_4Cl_{10}$.

Preparation

The pyridinium salt was synthesized by dissolving 1.21 g of $(4MAP)CuCl_3$[2] (0.005 mol) in 200 mL of 1-propanol, similarly dissolving 5.3 g (0.04 mol) of copper chloride in 150 mL of 1-propanol, and mixing. The green solution was filtered to remove excess copper chloride and slowly evaporated over low heat. A reddish brown precipitate was recovered by filtration and washed with cold 1-propanol. The crystals occurred in needlelike formation. Anal. Found, calcd: C, 17.48, 17.43; N, 6.66, 6.77; H, 2.75, 2.19.

The tetramethylammonium salt was prepared by dissolving a 1:2 ratio of (TEMA)Cl and $CuCl_2$ in hot concentrated HCl. Upon cooling, green chunky needle crystals precipitated. If necessary, additional $CuCl_2$ was added to avoid formation of the red needle crystals of $(TEMA)CuCl_3$. Large single crystals were readily grown by utilizing a temperature gradient technique.

Crystal Structure Determination

X-ray diffraction data collections were performed on a Nicolet R3m/E diffractometer system,[7] and the structures were solved by using direct methods within the Version 4.1 SHELXTL structure solution package.[8] As shown in Table I, $(4MAP)_2Cu_4Cl_{10}$ is monoclinic, $P2_1/n$, with a = 3.847 (2) Å, b = 21.276 (2) Å, c = 15.336 (6) Å, β = 96.44 (3)°, and Z = 2 for ρ_{calcd} = 2.20 g cm^{-3}. A numerical absorption correction (μ = 45.6 cm^{-1}) was applied for the room-temperature data collection, and a least-squares refinement on 121 parameters achieved a final R value of 0.068, with R_w = 0.077. The thermal parameters were anisotropic on all non-hydrogen atoms, while the hydrogen atoms were constrained to

(3) Willett, R. D. In *Magneto-Structural Correlations in Exchange Coupled Systems*; Willett, R. D., Gatteschi, D., Kahn, O., Eds.; NATO ASI Series C 140; Reidel: Dordrecht, The Netherlands, 1985; p 391.
(4) Grigereit, T.; Ramakrishna, B. L.; Place, H.; Willett, R. D.; Pellacani, G. C.; Manfridini, T.; Menabue, L.; Bonomartini-Corradi, A.; Battaglia, L. P. *Inorg. Chem.*, in press.
(5) Geoi, K.; Iizami, M. *J. Phys. Soc. Jpn.* **1980**, *48*, 1775. Sugiyama, J.; Wada, M.; Sawada, A.; Ishibashi, Y. *J. Phys. Soc. Jpn.* **1980**, *49*, 1405.
(6) Weenk, J. W.; Spek, A. L. *Cryst. Struct. Commun.* **1976**, *5*, 805.
(7) Campana, C. F.; Shephard, D. F.; Litchman, W. M. *Inorg. Chem.* **1981**, *20*, 4039.
(8) Sheldrick, G. "SHELXTL"; Nicolet Analytical Instruments: Madison, WI, 1984.

Table II. Atomic Coordinates (×10⁴) and Isotropic Thermal Parameters (Å² × 10³) for $(4MAP)_2Cu_4Cl_{10}$

atom	x	y	z	U[a]
Cu(1)	7724 (9)	305 (1)	4099 (2)	34 (1)
Cu(2)	3340 (9)	891 (1)	2230 (2)	33 (1)
Cl(1)	3058 (19)	1841 (3)	1616 (4)	38 (3)
Cl(2)	7281 (19)	1252 (3)	3423 (4)	37 (3)
Cl(3)	11913 (18)	650 (3)	5186 (4)	35 (2)
Cl(4)	3467 (17)	−39 (3)	3081 (4)	31 (2)
Cl(5)	−1137 (20)	493 (3)	1353 (4)	39 (3)
N(1)	6721 (66)	1555 (11)	9803 (13)	40 (9)
C(1)	6028 (63)	2160 (12)	8522 (15)	27 (10)
C(2)	4412 (94)	1679 (13)	8075 (16)	60 (14)
C(3)	3659 (86)	1089 (13)	8542 (18)	51 (12)
C(4)	5486 (93)	1066 (16)	9411 (21)	62 (15)
C(6)	7354 (81)	2060 (15)	9398 (18)	45 (13)
N(2)	8623 (80)	2576 (12)	9875 (18)	83 (13)
C(8)	2665 (106)	1695 (14)	7118 (16)	80 (16)

[a] The equivalent isotropic U is defined as one-third of the trace of the orthogonalized U_{ij} tensor.

Table III. Bond Lengths (Å) and Bond Angles (deg) for $(4MAP)_2Cu_4Cl_{10}$

A. Lengths

Cu(1)–Cl(2)	2.264 (7)	Cu(1)–Cl(3)	2.307 (7)
Cu(1)–Cl(4)	2.256 (7)	Cu(1)–Cl(3a)	2.260 (7)
Cu(2)–Cl(1)	2.226 (7)	Cu(2)–Cl(2)	2.372 (7)
Cu(2)–Cl(4)	2.371 (7)	Cu(2)–Cl(5)	2.231 (7)
Cu(2)–Cl(5a)	2.773 (8)		
N(1)–C(6)	1.279 (39)	N(1)–C(4)	1.268 (40)
C(1)–C(6)	1.401 (35)	C(1)–C(2)	1.346 (37)
C(2)–C(8)	1.547 (36)	C(2)–C(3)	1.490 (40)
C(6)–N(2	1.378 (40)	C(3)–C(4)	1.348 (42)

B. Angles

Cl(2)–Cu(1)–Cl(3)	93.4 (2)	Cl(2)–Cu(1)–Cl(4)	87.7 (2)
Cl(3)–Cu(1)–Cl(4)	177.5 (3)	Cl(2)–Cu(1)–Cl(3a)	178.6 (3)
Cl(3)–Cu(1)–Cl(3a)	86.3 (3)	Cl(4)–Cu(1)–Cl(3a)	92.6 (2)
Cl(1)–Cu(2)–Cl(2)	91.7 (2)	Cl(1)–Cu(2)–Cl(4)	171.2 (3)
Cl(2)–Cu(2)–Cl(4)	82.6 (2)	Cl(1)–Cu(2)–Cl(5)	95.3 (3)
Cl(2)–Cu(2)–Cl(5)	166.6 (3)	Cl(4)–Cu(2)–Cl(5)	89.0 (2)
Cl(1)–Cu(2)–Cl(5a)	94.3 (3)	Cl(2)–Cu(2)–Cl(5a)	90.9 (2)
Cl(4)–Cu(2)–Cl(5a)	92.5 (2)	Cl(5)–Cu(2)–Cl(5a)	99.9 (2)
Cu(1)–Cl(2)–Cu(2)	94.4 (2)	Cu(1)–Cl(3)–Cu(1a)	93.7 (3)
Cu(1)–Cl(4)–Cu(2)	94.6 (3)	Cu(2)–Cl(5)–Cu(2a)	99.9 (2)
C(4)–N(1)–C(6)	122.7 (25)	C(2)–C(1)–C(6)	118.2 (25)
C(1)–C(2)–C(3)	119.8 (23)	C(1)–C(2)–C(8)	126.6 (25)
C(3)–C(2)–C(8)	112.9 (24)	C(2)–C(3)–C(4)	112.0 (26)
N(1)–C(4)–C(3)	122.1 (28)	N(1)–C(6)–C(1)	121.8 (26)
N(1)–C(6)–N(7)	119.0 (24)	C(1)–C(6)–N(2)	117.3 (27)

C–H and N–H bond distances of 0.96 Å with isotropic thermal parameters fixed at approximately 1.2 times the corresponding heavy-atom thermal parameter. The largest peak on the final difference map was 0.8 e Å^{-3} near Cl(4). Atomic coordinates and thermal parameters are given in Table II, and bond distances and angles, in Table III.

Crystals of $(TEMA)_2Cu_4Cl_{10}$ grow as large, rather chunky dark needles. Small crystals are green in unpolarized light and exhibit a red–green pleochroism in polarized light. A crystal of dimensions 0.35 × 0.5 × 0.6 mm^3 was mounted on a glass fiber. The monoclinic unit cell for $(TEMA)_2Cu_4Cl_{10}$ has a = 6.072 (2) Å, b = 19.574 (3) Å, c = 10.617 (3) Å, and β = 99.46 (2)° with space group $P2_1/c$. Empirical absorption corrections (μ = 44.69 cm^{-1}) were made by assuming an ellipsoidally shaped crystal. Three standards were monitored every 100 reflections; corrections for a 5% decrease during the data collection were applied. Final refinement on F with anisotropic thermal parameters for the nonhydrogen atoms and isotropic thermal parameters for the hydrogen atoms gave final values of R = 0.039 and R_w = 0.035. The largest residual on the final difference map was approximately 0.67 e Å^{-3} near Cu(2). Final positional parameters are given in Table IV, with selected bond distances and angles reported in Table V.

Description of Structure

The structure of $(4MAP)_2Cu_4Cl_{10}$ consists of discrete $(Cu_4Cl_{10})^{2-}$ anions and $4MAP^+$ cations. Figure 1 shows the tetrameric unit. Each copper(II) ion within the tetramer has a near-square-planar coordination geometry, as seen in Figure 1.

Table IV. Atomic Coordinates (×10⁴) and Isotropic Thermal Parameters (Å² × 10³) for $[(CH_3)_4N]_2Cu_4Cl_{10}$

atom	x	y	z	U[a]
Cu(1)	3693 (1)	3991 (1)	1934 (1)	27 (1)
Cu(2)	8093 (1)	4660 (1)	801 (1)	28 (1)
Cl(1)	9354 (1)	5742 (1)	404 (1)	28 (1)
Cl(2)	5353 (2)	5067 (1)	1827 (1)	33 (1)
Cl(3)	6389 (2)	3633 (1)	807 (1)*U*	41 (1)
Cl(4)	8921 (2)	9467 (1)	2066 (1)	33 (1)
Cl(5)	3018 (2)	2936 (1)	2518 (1)	45 (1)
N	84898 (5)	1538 (2)	713 (3)	33 (1)
C(1)	8796 (8)	2068 (2)	−248 (4)	49 (2)
C(2)	7597 (8)	1854 (2)	1799 (4)	53 (2)
C(3)	10697 (7)	1215 (2)	1206 (4)	44 (1)
C(4)	6917 (7)	1004 (2)	103 (4)	50 (2)

[a] The equivalent isotropic U is defined as one-third of the trace of the orthogonalized U_{ij} tensor.

Table V. Bond Lengths (Å) and Bond Angles (deg) for $[(CH_3)_4N]_2Cu_4Cl_{10}$

A. Lengths

Cu(1)–Cl(2)	2.346 (1)	Cu(1)–Cl(3)	2.290 (1)
Cu(1)–Cl(5)	2.215 (1)	Cu(1)–Cl(4a)	2.252 (1)
Cu(2)–Cl(1)	2.315 (1)	Cu(2)–Cl(2)	2.278 (1)
Cu(2)–Cl(3)	2.260 (1)	Cu(2)–Cl(1a)	2.305 (1)
Cl(4)–Cu(1a)	2.252 (1)		
N–C(1)	1.487 (6)	N–C(2)	1.490 (6)
N–C(3)	1.493 (5)	N–C(4)	1.493 (5)

B. Angles

Cl(2)–Cu(1)–Cl(3)	84.2 (1)	Cl(2)–Cu(1)–Cl(5)	162.2 (1)
Cl(3)–Cu(1)–Cl(5)	92.4 (1)	Cl(2)–Cu(1)–Cl(4a)	89.6 (1)
Cl(3)–Cu(1)–Cl(4a)	173.1 (1)	Cl(5)–Cu(1)–Cl(4a)	94.4 (1)
Cl(1)–Cu8(2)–Cl(2)	93.2 (1)	Cl(1)–Cu(2)–Cl(3)	168.3 (1)
Cl(2)–Cu(2)–Cl(3)	86.5 (1)	Cl(1)–Cu(2)–Cl(1a)	86.5 (1)
Cl(2)–Cu(2)–Cl(1a)	174.9 (1)	Cl(3)–Cu(2)–Cl(1a)	92.8 (1)
Cu(1)–Cl(2)–Cu(2)	93.6 (1)	Cu(2)–Cl(1)–Cu(2a)	93.5 (1)
		Cu(1)–Cl(3)–Cu(2)	95.5 (1)
C(1)–N–C(2)	110.1 (3)	C(1)–N–C(3)	109.5 (3)
C(2)–N–C(3)	109.0 (3)	C(1)–N–C(4)	109.5 (3)
C(2)–N–C(4)	109.5 (3)	C(3)–N–C(4)	109.2 (3)

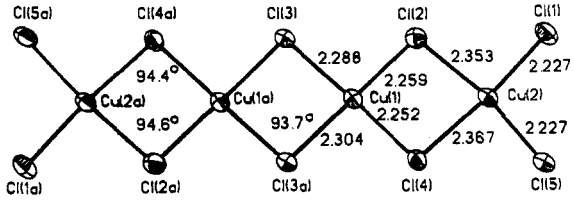

$(4MAP)_2Cu_4Cl_{10}$

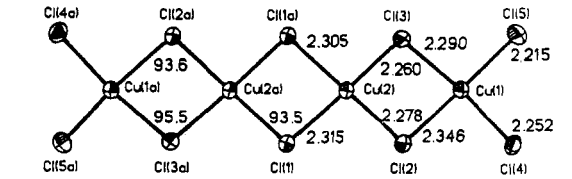

$(TEMA)_2Cu_4Cl_{10}$

Figure 1. Illustration of the $Cu_4Cl_{10}^{2-}$ anions in $(4MAP)_2Cu_4Cl_{10}$ and $(TEMA)_2Cu_4Cl_{10}$.

The Cu–Cl bond distances within the tetramer range from 2.227 to 2.367 Å, with an average of 2.285 Å. As expected, the terminal Cu–Cl bond distances are shorter than the bridging distances. In addition, a trans effect causes the Cu–Cl bonds that are trans to the terminal Cu–Cl bonds to be abnormally long. The interior Cl–Cu–Cl angles are all typically less than 90°. The magnetically

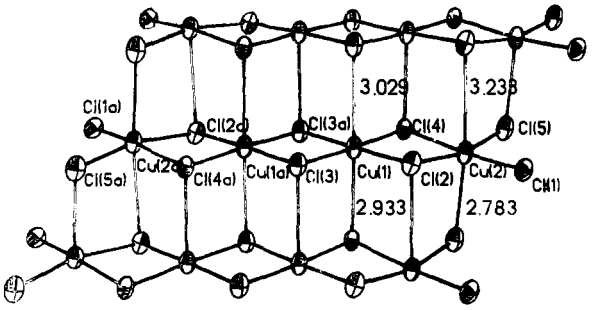

Figure 2. Stacking of the $Cu_4Cl_{10}^{2-}$ tetramers in $(4MAP)_2Cu_4Cl_{10}$.

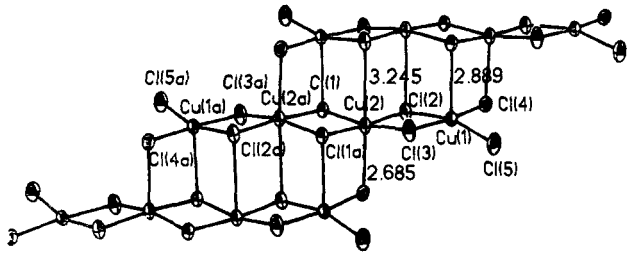

Figure 3. Stacking of the $Cu_4Cl_{10}^{2-}$ tetramers in $(TEMA)_2Cu_4Cl_{10}$.

important Cu–Cl–Cu bridging angles average 94.5° for the terminal pairs and 93.7° for the central pair. The tetramer is pseudoplanar, with significant deviations from the least-squares plane occurring only at the Cu(2) atoms. The displacement of the end copper atoms out of the least-squares plane is due to the bifurcated hydrogen bonding of N(2) to Cl(5) and Cl(2), which have typical N–Cl bond lengths of 3.32 (9) and 3.31 (9) Å, respectively.

The anions and cations form segregated stacks along the crystallographic *a* axis, as shown in Figure 2. Each copper ion in a tetramer forms two semicoordinate bonds to chloride ions in adjacent tetramers to yield a 4 + 2 coordination geometry. The semicoordinate distances range from 2.783 to 3.216 Å, with the shortest distances at the end of the tetramer. This is due to the tipping of Cl(5) toward Cu(2). The stacking pattern is designated as $4(^1/_2,^1/_2)$ in the notation of ref 9. These stacks can be viewed as short segments of the $CuCl_2$ chain.[10] Therefore, the role of the cations is to interrupt the infinite chains in $CuCl_2$ and to provide a countercharge to the anions thus formed.

The structure of $(TEMA)_2Cu_4Cl_{10}$ (Figure 3) consists of discrete centrosymmetric $Cu_4Cl_{10}^{2-}$ anions and $TEMA^+$ cations. The stacking pattern is $4(^3/_2,^1/_2)$, in the notation of ref 9, for which the two end copper(II) ions have a 4 + 1 coordination geometry, while the two central copper(II) ions have a 4 + 2 coordination geometry. The stacking is parallel to the *a* axis. The Cu–Cl distances within the tetramers are all normal, ranging from 2.260 to 2.346 Å for the bridging Cu–Cl distances (average 2.298 Å) and from 2.215 to 2.252 Å for the terminal Cu–Cl distances (average 2.233 Å). The bridging Cu–Cl–Cu angles, of interest magnetically, are 93.5° for the central Cu(2)–Cl(1)–Cu(2) bridges and 93.6 and 95.5° (average 94.6°) for the Cu(1)–Cl–Cu(2) bridges. The semicoordinate copper–chlorine distances between tetramers range from 2.635 to 3.245 Å, with the longest distances to the interior chloride ions. Cl(5) is tipped considerably out of the least-squares plane of the tetramer toward Cu(2), leading to that particularly short distance. The distances and angles in the TEMA ion are normal (N–C = 1.491 Å average; C–N–C = 109.2–110.1°). The TEMA ions are located at the ends of each tetramer, terminating the oligomers and providing charge compensation for the nonbridging chloride ions.

The variety of stacking arrangements in copper(II)–halide bibridged oligomers can be seen from a comparison of the 4MAP and TEMA tetramers reported here to the $[(CH_3)_3NH]_2Cu_4Cl_{10}$ tetramer[11] and the $[(CH_3)_3NH]_2Cu_4Br_{10}$ tetramer,[9] which stack in patterns II and III, respectively. This variety is due to the

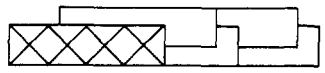

III

versatility of copper(II) coordination geometry[3] and to the hydrogen bonding and charge compensation effects of the organic cations present.[12]

Magnetic Analysis

Powder magnetic susceptibility measurements on the two tetramers were made in the temperature range of 5–300 K with a PAR vibrating-sample magnetometer. The background moments were determined and subtracted from those of the compounds. The data were also corrected for temperature-independent paramagnetism and diamagnetism.[13]

On the basis of the crystal geometry, the data were fit to a nearest-neighbor Heisenberg Hamiltonian for a linear tetramer

$$\mathcal{H} = -2J_1(\vec{s}_1\cdot\vec{s}_2 + \vec{s}_3\cdot\vec{s}_4) - 2J_2(\vec{s}_2\cdot\vec{s}_3)$$

where J_1 is the exchange constant between the outer pair of copper(II) ions and J_2 is the central exchange constant. This model has been solved exactly elsewhere,[14] and the magnetic susceptibility is given as

$$\chi_m = (N_0g^2\mu_B^2/kT)[10\exp(-E_1/kT) + 2\exp(-E_2/kT) + 2\exp(-E_3/kT) + 2\exp(-E_4/kT)][(1-x)/Z] + xN_0g^2\mu_B^2/kT \quad (1)$$

where Z is the partition function, x is the fraction of the sample appearing as an impurity, and the energy levels and spin quantum numbers are

$$E_1 = -J_1 - (1/2)J_2 \qquad S_1 = 2$$

$$E_2 = J_1 - (1/2)J_2 \qquad S_2 = 1$$

$$E_3 = (1/2)J_2 + [J_1^2 + J_2^2]^{1/2} \qquad S_3 = 1$$

$$E_4 = (1/2)J_2 - [J_1^2 + J_2^2]^{1/2} \qquad S_4 = 1$$

$$E_5 = J_1 + (1/2)J_2 + [4J_1^2 - 2J_1J_2 + J_2^2]^{1/2} \qquad S_5 = 0$$

$$E_6 = J_1 + (1/2)J_2 - [4J_1^2 - 2J_1J_2 + J_2^2]^{1/2} \qquad S_6 = 0$$

The results of the fit of the data to the model for the 4MAP salt are shown in Figure 4, with $J_1/k = -62.1$ (2) K, $J_2/k = 36$ (33) K, $g = 2.16$ (2), and the fraction of impurity $x = 0.042$ (3). Strong antiferromagnetic coupling exists between the outer pairs of copper atoms. The coupling between the central pair is poorly defined because, as the temperature is lowered, the tetramer initially decouples magnetically into two dimers consisting of the two outer pairs of copper(II) atoms. With only the $S = 0$ ground state in each "dimer" being appreciably populated, the interaction between the "dimers" is negligible and thus the data are insensitive to the value of J_2/k within the limits indicated above. This strong coupling between the outer pairs explains the approach of χT to zero as the temperature approaches zero, since the antiferromagnetic ground states of the "dimers" dominate the magnetic response of the compound. A plot of $\chi_m T$ vs. T for $(TEMA)_2Cu_4Cl_{10}$ is shown in Figure 4. The solid line is the fit to eq 1 with $J_1/k = -59.2$ (9) K, $J_2/k = 26$ (18) K, and $g = 2.09$ (1) and with an impurity fraction of $x = 0.0286$ (9).

(9) Geiser, U.; Willett, R. D.; Lindbeck, M.; Emerson, K. *J. Am. Chem. Soc.* **1986**, *108*, 1173.
(10) Wells, A. F. *J. Chem. Soc.* **1947**, 1670.
(11) Caputo, R. E.; Vukosavavich, M. J.; Willett, R. D. *Acta Crystallogr., Sect. B: Struct. Crystallogr. Cryst. Chem.* **1976**, *B32*, 2516.
(12) Willett, R. D.; Geiser, U. *Croat. Chem. Acta* **1985**, *57*, 737.
(13) König, E.; König, G. *Landolt-Börnstein, Zahlenwerte und Funktionen aus Naturwissenschaften und Technik*; Springer: Berlin, Heidelberg, New York, 1976; New Series, Vol. II/8, p 27.
(14) Rubenacker, G. V.; Drumheller, J. E.; Emerson, K.; Willett, R. D. *J. Magn. Magn. Mater.* **1986**, *54–57*, 1483.

Table VI. Structural and Magnetic Data for Pseudoplanar $Cu_nX_{2n+2}^{2-}$ Oligomers

compd	X = Cl⁻ Cu–Cl–Cu angle ϕ, deg	X = Cl⁻ Cu–Cl dist (bridging), Å	X = Cl⁻ J/k, K	X = Br⁻ Cu–Br–Cu angle ϕ, deg	X = Br⁻ Cu–Br dist (bridging), Å	X = Br⁻ J/k, K
		Dimers (n = 2)				
$KCuX_3$[a]	95.5	2.318	−28			−95
(melaminium)Cu_2X_6[b]	95.8	2.334	−28	95.6	2.468	−113
		Trimers (n = 3)				
$(3MAP)_2Cu_3Cl_8$[c]	93.6	2.321	−30			
(N-Mepipz)Cu_3Cl_8[c]	94.20	2.284	−26			
(N-Mephen)Cu_3Cl_7·EtOH[c]	94.0	2.301	−32			
$(Et_2NH_2)_2Cu_3Br_8$·$CuBr_2$·EtOH[d]				94.4	2.442	−100
		Tetramers (n = 4)[g]				
$(4MAP)_2Cu_4Cl_{10}$[e]	94.5	2.276	−62			
$(Me_4N)_2Cu_4Cl_{10}$[e]	94.6	2.294	−60			
$(Me_3NH)_2Cu_4Br_{10}$[f]				94.8	2.445	−180
		Infinite Chains				
CuX_2[h]			−54	92.1	2.413	−165

[a] Willett, R. D. *Inorg. Chem.* [b] Colombo, A.; et al. *Inorg. Chem.* **1985**, *24*, 2900. Pellacani, G. C., private communication. [c] Grigereit, T.; et al. *Inorg. Chem.*, in press. [d] Fletcher, R.; et al. *Inorg. Chem.* **1983**, *22*, 330. [e] This work. [f] Geiser, U.; et al. *J. Am. Chem. Soc.* **1986**, *108*, 167. [g] Terminal bridges. [h] Halverson, K., private communication.

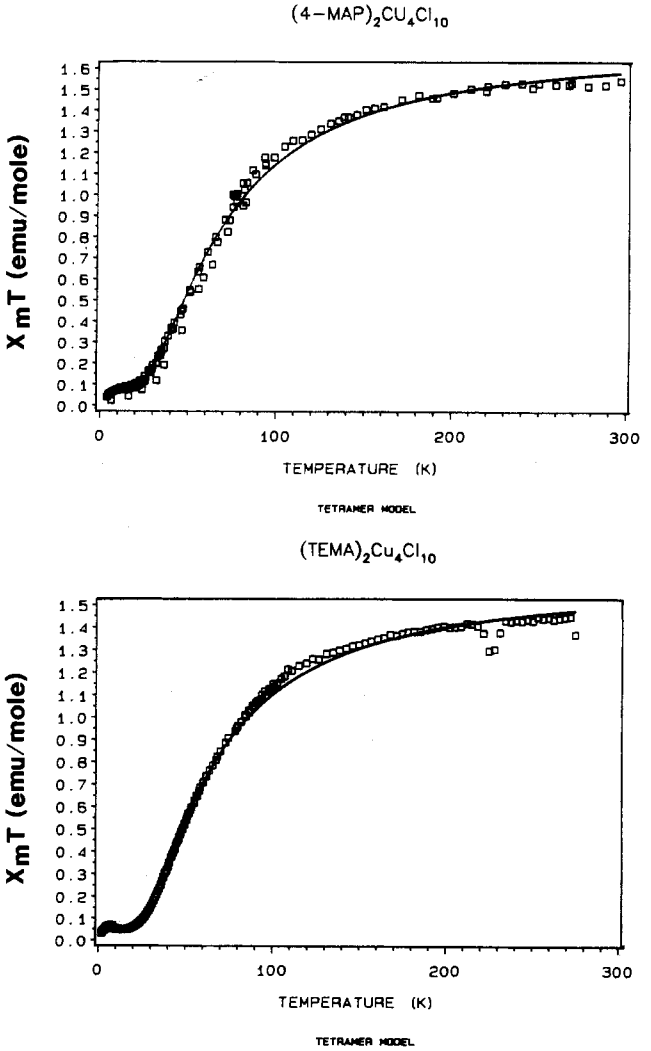

Figure 4. Plots of χT vs. T for $(4MAP)_2Cu_4Cl_{10}$ and $(TEMA)_2Cu_4Cl_{10}$.

Examination of the fit of eq 1 to the data for each compound reveals systematic deviations from ideal Boltzmann behavior, with the calculated values of χT being too high at high temperature and dropping too low in the intermediate temperature regime. Thus, the depopulation of the higher spin states as temperature is lowered occurs more slowly than predicted by eq 1. In a study of $Cu_3Cl_8^{2-}$ trimeric systems,[4] this was attributed to the phenomenon of partial spin frustration, caused by interoligomer interactions, which leads to stabilization of the excited quartet state. In the trimeric systems, it was possible to model this in a phenomenological fashion with a simple mean field correction to that highest spin state. Extension of that approach to the tetrameric systems is not possible, since interactions between all of the nonzero spin states would have to be accounted for. Nevertheless, it is clear that such interactions would lead to a quantitatively better fit of the data, but as with the trimeric systems, the value of J_1 would not be appreciably affected.

Comparison with other pseudoplanar $Cu_nX_{2n+2}^{2-}$ oligomers (Table VI) reveals some very interesting, but unexpected, trends. It is observed that J tends to become more negative as n increases. In planar bibridged Cu(II) systems, the exchange coupling is normally correlated with the bridging Cu–X–Cu angle, ϕ, with J becoming more antiferromagnetic as ϕ increases from 90°.[15,16] From Table VI, it is seen that the compound with the smallest angle, $CuBr_2$, ϕ = 92.1°, has one of the strongest antiferromagnetic coupling constants, J/k = −165 K. Thus, additional factors must be operative. One parameter of significance is certainly the Cu–X bond lengths in the bridge, since the delocalization of the magnetic electron out onto the ligands decreases as the Cu–X distance increases. Thus, shorter distances should lead to stronger antiferromagnetic coupling due to increased overlap. The bridging Cu–X bond lengths in dimeric species are particularly long, since the trans effect of the shorter terminal Cu–X bonds causes *all* bridging bonds to be elongated. In trimers and tetramers, only half of the bridging Cu–X distances are elongated. Other effects must account for the difference between the exchange coupling for the trimers and the terminal bridges in the tetramer, as well as for the infinite chains. Possible effects include the unusually large terminal X–Cu–X angle, variations in the semicoordinate Cu···X distances, and small deviations from nonplanarity. Theoretical calculations to explore these factors are planned.

Acknowledgment. The support of NSF Grant DMR-8219430 is gratefully acknowledged. The X-ray diffraction facility was established in part through funds from NSF Grant CHE-8408407 and from the Boeing Co.

Supplementary Material Available: Tables of thermal parameters and derived hydrogen positions and unit cell packing diagrams for $(4MAP)_2Cu_4Cl_{10}$ and $[(CH_3)_4N]_2Cu_4Cl_{10}$ (4 pages); listings of calculated and observed structure factors for both compounds (10 pages). Ordering information is given on any current masthead page.

(15) Hay, P. J.; Thiebault, S. C.; Hoffmann, R. *J. Am. Chem. Soc.* **1975**, *97*, 4884.
(16) Hatfield, W. E. In *Magneto-Structural Correlations in Exchange Coupled Systems*; Willett, R. D., Gatteschi, D., Kahn, O., Eds.; NATO ASI Series C 140; Reidel: Dordrecht, The Netherlands, 1985; p 555.